

Fabry-Perot Lasers in Simultaneous Strain and Temperature Brillouin-based Distributed Sensing

M. A. Soto, G. Bolognini, F. Di Pasquale

Scuola Superiore Sant'Anna, via G. Moruzzi 1, 56124, Pisa, Italy; email: gabriele.bolognini@sssup.it

Abstract *The use of Fabry-Perot lasers is proposed for simultaneous strain and temperature sensing based on spontaneous Brillouin scattering. A significant sensing performance enhancement is achieved compared to the use of single-longitudinal mode lasers.*

Introduction

Distributed Brillouin-based optical fiber sensors have been widely reported in recent years due to their possibilities to perform distributed strain and temperature sensing along an optical fiber [1,2], providing an interesting sensing mechanism for structural-health monitoring and several other sensing applications. While sensors based on stimulated Brillouin scattering (SBS) require the access to both fibre-ends [1] and the use of two optical fibres to distinguish between strain and temperature effects, sensors based on spontaneous Brillouin scattering (SpBS) require the access to a single fibre-end and allow one to overcome the strain-temperature cross-sensitivity by measuring simultaneously the SpBS intensity and frequency shift (BFS) parameter [2].

In this paper we propose the use of multi-wavelength Fabry-Perot (FP) lasers to improve the sensing performance of SpBS-based sensors. Using FP lasers overcomes the maximum input power limitation imposed by the onset of nonlinearities, also allowing for an efficient exploitation of optical pulse coding techniques for further strain and temperature sensing enhancement [3,4].

Theory

In SpBS-based sensors the SpBS intensity (ΔP_B) and BFS ($\Delta \nu_B$) are both linearly dependent on strain and temperature; this makes the simultaneous strain ($\Delta \epsilon$) and temperature (ΔT) sensing along a single optical fiber possible by using the following matrix relation:

$$\begin{bmatrix} \Delta \nu_B \\ \Delta P_B \end{bmatrix} = \begin{bmatrix} C_{\nu_B \epsilon} & C_{\nu_B T} \\ C_{P_B \epsilon} & C_{P_B T} \end{bmatrix} \begin{bmatrix} \Delta \epsilon \\ \Delta T \end{bmatrix} \quad (1)$$

where $C_{\nu_B \epsilon} = 0.046 \text{ MHz}/\mu\epsilon$, $C_{\nu_B T} = 1.07 \text{ MHz}/^\circ\text{C}$, $C_{P_B \epsilon} = 8 \cdot 10^{-4} \text{ } \%/ \mu\epsilon$ and $C_{P_B T} = 0.36 \text{ } \%/ ^\circ\text{C}$ are the strain and temperature coefficients for BFS and SpBS power [2]. The performance of SpBS-based sensors is ultimately limited by the SBS threshold, which imposes the maximum peak power allowed at fibre input. We have recently demonstrated that the use of optical pulse coding allows for a simultaneous strain and temperature sensing improvement [4], reducing the SBS threshold depending on the code length.

Compared to single-longitudinal mode lasers, such as distributed feedback (DFB) or external cavity lasers (ECL), FP lasers can in principle offer several advantages for sensing applications: 1) They typically provide higher optical power; 2) The total power in FP

lasers is spectrally distributed among several longitudinal modes, thus possibly increasing the SBS threshold in an effective way (the SBS threshold, due to narrowband Brillouin gain, actually constraints the FP power per mode and not total power); 3) Due to their large spectrum (typically several nm), FP lasers allow for accurate Rayleigh-scattering (RS) measurement (required to normalize the SpBS intensity), suppressing coherent-Rayleigh noise (CRN) and avoiding current dithering or λ -averaging techniques [5]. Thus in this paper we propose the use of multi-longitudinal-mode FP lasers for simultaneous temperature and strain sensing based on SpBS. In order to measure both SpBS intensity and BFS, a coherent-detection scheme is required [2]; the Brillouin signal is mixed with an optical local oscillator (OLO), providing amplification of the weak SpBS signal, efficient spectral filtering and higher dynamic range compared to direct-detection schemes.

Note that when a FP laser is coupled into a sensing fibre, each longitudinal mode generates different SpBS signals. In order to efficiently exploit all Brillouin components, a coherent-detection scheme with a multi- λ OLO is required. This can actually be obtained by splitting a portion of the same FP laser light, so that the beating of each FP mode with the respective Stokes and anti-Stokes components generates an electric signal around the BFS. Thus, the contribution of all FP modes provides an enhanced performance in comparison to single-longitudinal mode lasers.

Experimental set-up

The experimental set-up is shown in Fig. 1. DFB and FP lasers are alternatively employed so that their sensing performances can be compared. Note that, while current dithering is required when using DFB lasers to reduce CRN effects in RS measurements, this can be avoided when employing FP lasers thanks

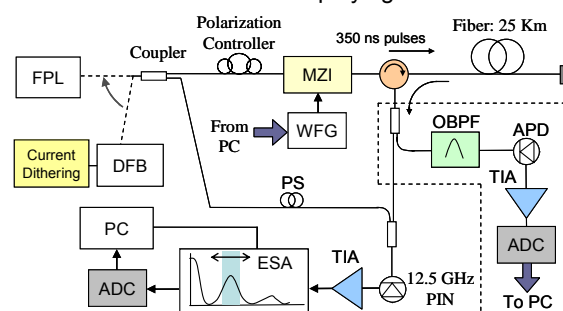


Fig. 1: Experimental setup

to their broad optical spectrum suppressing CRN effects [5]. The CW-light of the source is split into two parts using an optical coupler; 10% of the light is used as OLO at the receiver side, whereas the 90% is modulated, by using a Mach-Zehnder interferometer (MZI), with 127-bit Simplex-coded pulses. The DFB laser, operating at 1550 nm, allows for a maximum power of 1.5 dBm at the fibre input after the MZI (a typical value for DFB), whereas the FP laser (centred at 1545 nm, 10 nm linewidth) allows for 15 dBm at the fibre input (also a typical value for FP lasers). The pulse duration is 350 ns, allowing for 35 m spatial resolution. Optical pulses are launched into 25 km of standard single mode fiber, and the backscattered light is then coupled into the receiver side, which is composed by two stages. The first one is a direct-detection receiver used for Rayleigh measurement and consists in a PIN photodiode, followed by a trans-impedance amplifier (TIA) and analog-digital converter (ADC) connected to a computer (PC). The second stage is a heterodyne receiver, where the OLO is mixed with the Brillouin components backscattered from the sensing fibre. Signals are detected by using a 12.5 GHz PIN, followed by a TIA and a 40 GHz electrical spectrum analyser (ESA) operating in zero-span mode. To reduce polarization-induced noise, the OLO has been depolarized by using a polarization scrambler (PS) reducing its degree of polarization down to less than 1%.

Results

Fig. 2 reports a zoom of the FP laser spectrum where three longitudinal modes and the respective backscattered components (Rayleigh, Brillouin Stokes and anti-Stokes) from the sensing fiber are shown. The linewidth of each FP mode results significantly narrower than the Brillouin gain bandwidth. This and the large spectral separation among adjacent modes (~0.3 nm which is more than twice the BFS in silica), allow us to clearly observe and measure the Brillouin-scattered components for each FP longitudinal mode. The electrical signal at ~10.9 GHz from the PIN in Fig. 1, representing the summed contribution of Stokes and anti-Stokes components generated by all FP longitudinal modes, is measured by operating the ESA in zero-span mode, with a resolution bandwidth of 3 MHz [2,4], achieving an enhanced SNR with respect to the detection of a single-longitudinal mode.

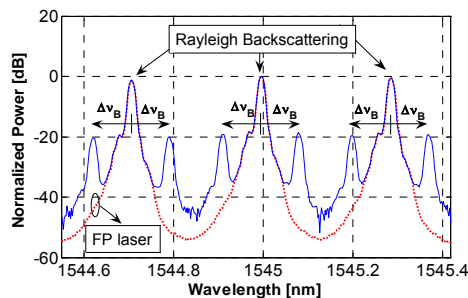


Fig. 2: Optical spectrum of the FP laser and respective Rayleigh, Brillouin Stokes and anti-Stokes components

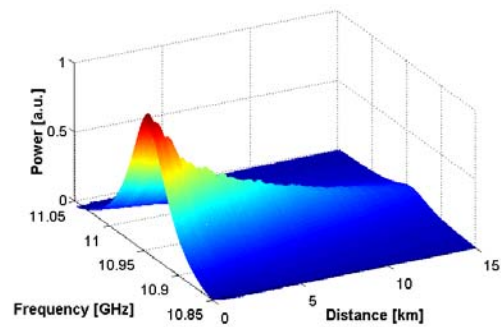


Fig. 3: Brillouin spectrum vs distance

The final BFS parameter is then obtained by fitting the measured spectrum (averaged and decoded from 128K SpBS-trace acquisition) with a Lorentzian curve at each fiber position. Note that the measured Brillouin spectrum using FP laser (shown in Fig. 3) does not show any distortion along the fiber, even if the total input power (15 dBm) is higher than the SBS threshold for single-mode lasers with coding (~10 dBm as reported in [3]). The SpBS intensity (obtained simply by spectrum integration) and BFS are then used in Eq (1) to compute the distributed strain and temperature resolutions reported in Fig. 4. The achieved temperature resolution is reduced from ~20 K (obtained with the DFB laser at 25 km

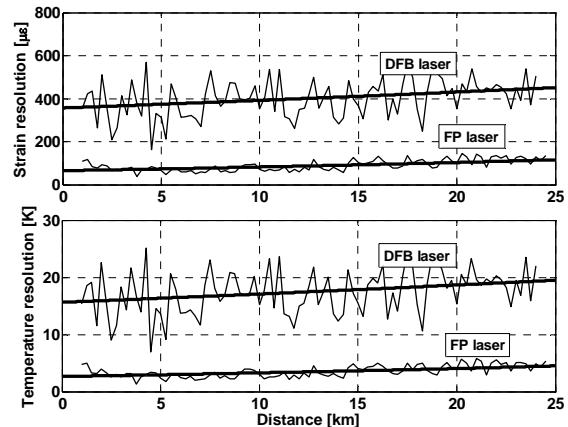


Fig. 4: Achieved strain and temperature resolution

distance) down to ~4.5 K when using the FP laser, whereas the strain resolution is improved from ~450 με down to ~115 με. These results clearly point out the potential of using standard FP lasers for performance improvement in SpBS-based sensors, especially in combination with optical pulse coding. In conclusion, we have shown that the FP laser longitudinal modes structure allows for a significant performance improvement in SpBS-based sensors with respect to the typically used DFB lasers.

References

1. X. Bao et al., Opt. Lett. **19**, 141-143 (1994).
2. S. Maughan et al., Meas. Sci. Technol. **12**, 834-842 (2001).
3. M. A. Soto et al., Opt. Express **16**, 19097-19111 (2008).
4. M. A. Soto et al., IEEE PTL **21**, 450-452 (2009).
5. K. De Souza, Meas. Sci. Technol. **17**, 1065-1069 (2006).